buildings

MDPI

Article

Machine Learning Prediction and Evaluation for Structural Damage Comfort of Suspension Footbridge

Shaojie Zhao [1,*], Xing Tang [1,*] and Yongjun Du [2]

[1] School of Civil Engineering, Xiangtan University, Xiangtan 411105, China
[2] Shanxi Xingtong Engineering Consulting Co., Ltd., Xi'an 710061, China; 202121572186@smail.xtu.edu.cn
* Correspondence: shaojiez@xtu.edu.cn (S.Z.); 202121572156@smail.xtu.edu.cn (X.T.)

Abstract: To investigate the impact of structural damages on the comfort level of suspension footbridges under human-induced vibrations, this study addresses the limitations of traditional manual testing, which often entails significant manpower and material resources. The aim is to achieve rapid estimation and health monitoring of comfort levels during bridge operation. To accomplish this, the study combines finite-element simulation results to establish a data-driven library and introduces three distinct machine learning algorithms. Through comparative analysis, a machine learning-based method is proposed for quick evaluation of bridge comfort levels. Focusing on the Yangjiadong Suspension Bridge, the study evaluates and researches the comfort level of the structure under the influence of human-induced vibrations. The findings revealed a relatively low base frequency and high flexibility. Additionally, when considering the mass of individuals, peak acceleration decreased. The predictive performance of the Artificial Neural Network (ANN) model was found to be superior when accounting for multi-parameter damages, yielding root mean square error (*RMSE*), mean absolute percentage error (*MAPE*), and R-squared (R^2) values of 0.03, 0.02, and 0.98, respectively. Moreover, the error ratio of the generalization performance analysis was below 5%. Furthermore, the study identified a damage coefficient of 0.13 for the bridge's main cable, hanger, and steel longitudinal beam. Under a crowd density of 0.5 people per square meter, the predicted peak acceleration was 1.098 m/s^2, with a model error of less than 10% compared to the observed value of 1.004 m/s^2. These results underscore the model's effectiveness in swiftly evaluating bridge comfort levels, thereby offering valuable insights for the health monitoring of bridge comfort levels.

Keywords: safety engineering; suspension footbridge; human-induced vibration; comfort level evaluation; machine learning; structural damage

Citation: Zhao, S.; Tang, X.; Du, Y. Machine Learning Prediction and Evaluation for Structural Damage Comfort of Suspension Footbridge. *Buildings* **2024**, *14*, 1344. https://doi.org/10.3390/buildings14051344

Academic Editor: Alireza Entezami

Received: 26 March 2024
Revised: 27 April 2024
Accepted: 7 May 2024
Published: 9 May 2024

1. Introduction

The suspension bridge stands as a crucial component in contemporary transportation infrastructure. Suspension footbridges, a variation of these structures, primarily serve pedestrian traffic. However, they differ in control loads and structural characteristics from highway suspension bridges. Designed with aesthetics in mind, these footbridges often prioritize "lightness" and "flexibility", which may result in increased vibrations under pedestrian loads. These vibrations not only impact pedestrian comfort but can also pose security risks to the structure in extreme cases. Thus, assessing the comfort and safety levels of suspension footbridges under human-induced vibrations emerges as a pivotal area of study.

As mentioned in the review of Zivanovic et al. [1], in 1931, two German scholars, Reiher and Meister, first conducted systematic research on vibration comfort levels. Through experiments, their study utilized researchers' subjective perceptions to categorize comfort levels into seven distinct levels, establishing a foundational framework for subsequent investigations. Subsequent researchers conducted a series of experiments and studies. In 1961, Harper et al. [2,3] utilized a single-board force platform to conduct the first-ever test

on the load generated by single-person walking. They concluded that the vertical component force and the time curve exhibited a distinct double-peak pattern. In 1963, Wright and Green [4] measured the peak vibration of 52 bridges and, based on this, proposed the concept of comfort limit classification. Employing on-site testing methodologies, Lai et al. [5] performed modal analysis on a steel suspension footbridge and examined its dynamic response under pedestrian loads. Similarly, taking the Chulitna River Bridge as the engineering background, Feng et al. [6] used finite-element software to analyze the modal parameters and dynamic response of the bridge structure under specific ambient loading and compared it with the field measurement results. Feng Peng et al. [7] conducted a comprehensive questionnaire survey on 21 passenger footbridges in Beijing. They introduced comfort level coefficients and perception coefficients, establishing the relationship between these coefficients and the span of the bridges. Han et al. [8] conducted an analysis and study on the mechanism of horizontal human–bridge sympathetic vibration through modeling analysis. They deduced the equation of non-linear time-variant motion and proposed a horizontal vibration model for the process of two-way pedestrian bridge passing. Yu Zhenghua et al. [9], through theoretical analysis of the time domain of the bridge's dynamic response, evaluated and researched the performance of cable-stayed bridges against vibrations and their comfort level under the combined influence of wind, vehicles, and crowds. Liu Feng et al. [10] undertook research on vibration responses influenced by excitation parameters caused by different crowds. They employed a method combining practical measurement and finite-element simulation and suggested a damping value range of 0.2–0.4% based on an analysis of general suspension footbridges' human-induced vibrations. Zhang Yanling et al. [11] analyzed the response to human-induced vibrations and the comfort level of suspension bridges with two different suspender forms: vertical and tilted. Their research indicated that the model with tilted suspenders performed better. Additionally, researchers have conducted numerous studies on measures for vibration reduction and inhibition [12,13].

The application and development of computer vision and machine learning methods offer a novel approach to evaluating the comfort level of footbridges against vibration. Bayane et al. [14] integrated the three factors of strain, acceleration, and environmental change, proposing a real-time bridge damage detection method based on a machine learning algorithm. Chen et al. [15], in their effort to predict and evaluate the performance of lightweight foamed concrete, constructed three machine learning models for comparative analysis. The findings revealed that the amalgamation of these three machine learning models yielded the highest accuracy. Dong et al. [16] proposed a computer-aided visible method for assessing footbridge comfort against vibration. Building upon walking tests and a combination of theoretical analysis and intelligent identification algorithms, Cao Liang et al. [17] introduced an algorithm for determining human body kinetic parameters during walking, which is utilized to assess the structural comfort level induced by human activity. Chen et al. [18] introduced a real-time system capable of assessing footbridge vibration comfort levels in response to human-induced vibrations, leveraging smart devices as the basis of their approach.

In conclusion, numerous studies have been conducted both domestically and internationally on assessing the comfort level against human-induced vibrations, covering areas such as the walking load model, mechanisms of human–bridge sympathetic vibration, and analysis of comfort levels based on the coupling of multiple loads. However, there remains a scarcity of research that integrates machine learning for evaluating structural comfort levels. Incorporating machine learning algorithms into comfort level evaluations can effectively address shortcomings inherent in traditional artificial testing, such as excessive manpower and material resource consumption. Building upon this premise, this study focused on the suspension footbridge in Yangjiadong as its engineering context. Data for model training were acquired through finite-element modeling, and three distinct machine learning models were developed using different algorithms. Subsequently, evaluation indicators, including root mean square error (*RMSE*), mean absolute percentage error

(*MAPE*), and coefficient of determination (R^2), were employed to assess the performance of these models. The model demonstrating the most favorable evaluation performance was selected, and a method for rapidly evaluating the suspension footbridge's comfort level based on machine learning was proposed. The results indicated that the proposed method exhibits high precision and satisfactory generalization performance. The *RMSE*, *MAPE*, and R^2 values for the validation set were 0.03, 0.02, and 0.98, respectively, with the error in generalization performance analysis remaining below 5%. Consequently, this method can be effectively utilized for quickly evaluating the comfort level against human-induced vibrations of suspension footbridges afflicted by multi-parameter damages and, at the same time, it provides a reference for the comfort level health monitoring of bridges.

2. Comfort Level Evaluation and Procedure

2.1. Pedestrian Load Calculation

The research employed the calculation method outlined in the Germany EN03 norm [19]. The horizontal first-order stride frequency of pedestrians ranges from 0.5 Hz to 1.2 Hz, while the vertical first-order stride frequency ranges from 1.25 Hz to 2.3 Hz. Considering that the base frequency of the bridge's structure falls within the range of pedestrian first-order stride frequencies, it is necessary to calculate the structure's dynamic response. The modal frequency of the bridge's base within the pedestrian's first-order stride frequency range was selected to analyze the dynamic response of the structure, utilizing Formula (1). To account for the periodic nature of pedestrian load, the actual pedestrian load was treated as equivalent to a periodic pedestrian load model:

$$P(t) = P_0 cos(2\pi f \cdot t) n' \psi \tag{1}$$

In this formula: The symbol $P(t)$ stands for the simple harmonic wave load. The symbol P_0 stands for the component of the load generated by a single pedestrian. The horizontal P_0 is taken as 35 N, and the vertical P_0 as 280 N. The symbol f stands for the natural vibration frequency, the symbol t stands for the time, and the symbol n' stands for the equivalent number of pedestrians on the bearing surface S. When the number of pedestrians within the unit area is smaller than 1, $n' = 10.8\sqrt{\xi n}/S$. When the number is larger than or equal to 1, $n' = 1.85\sqrt{n}/S$, in which ξ stands for the damping coefficient of the structure. The value of the steel-structure bridge is taken as 0.02, and S is the area of the bridge's surface. The symbol ψ stands for the reduction coefficient of the amplitude variation caused by different pedestrian frequencies. The selected values are shown in Figure 1.

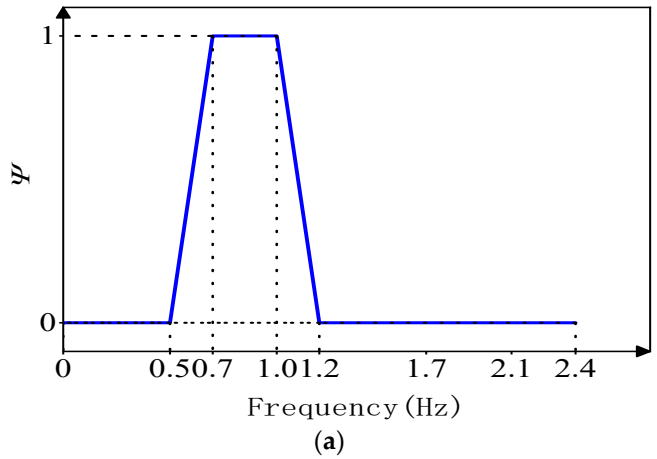

(**a**)

Figure 1. *Cont.*

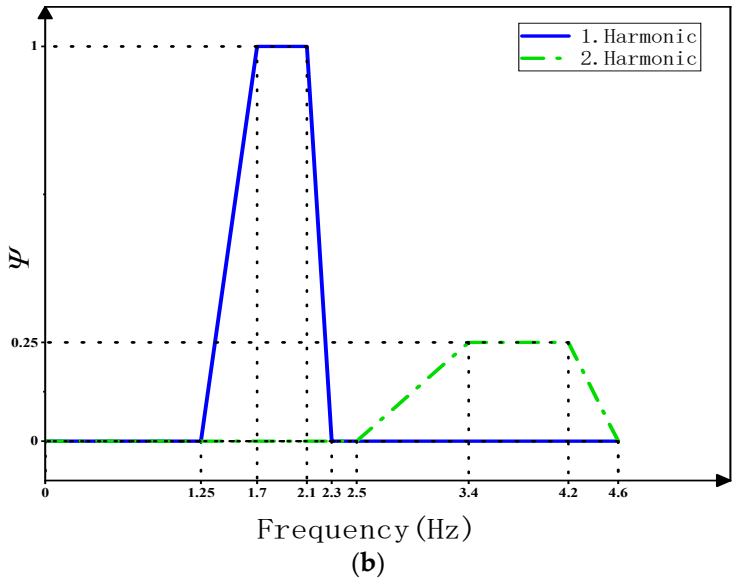

(**b**)

Figure 1. Reduction coefficients, Ψ. (**a**) Horizontal vibrations and (**b**) vertical and longitudinal vibrations.

In addition, the Germany EN03 norm [19] also stipulates the loading method of the pedestrian load model. It loads the equivalent periodic pedestrian load model in accordance with specific vibration modes in the form of uniformly distributed loads. The loading diagram is shown in Figure 2.

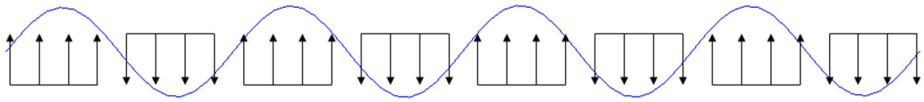

Figure 2. Loading method of the pedestrian load model.

2.2. Evaluation Standard of the Comfort Level

According to the Germany EN03 norm [19], we evaluated the comfort level of the suspension bridge, adopted the method of dynamic response value restriction to conduct dynamic response analysis, and classified the grade of the comfort level in accordance with the result of the dynamic response analysis in a detailed form, as specifically shown in Table 1.

Table 1. Comfort level evaluation standard of the EN03 norm.

Comfort Level Grade	Comfort Level Degree	Limited Value of Horizontal Acceleration (m/s^2)	Limited Value of Vertical Acceleration (m/s^2)
1	Very Comfortable	<0.1	<0.5
2	Intermediate Comfort Degree	0.1~0.3	0.5~1.0
3	Uncomfortable	0.3~0.8	1.0~2.5
4	Unacceptable	>0.8	>2.5

2.3. Construction of the Machine Learning Evaluation Model

2.3.1. Machine Learning Algorithm Selection

In this study, we employed three machine learning algorithms: eXtreme Gradient Boosting (XGBoost), Support Vector Regression (SVR), and Artificial Neural Network (ANN), to develop an evaluation model for assessing the comfort level of suspension footbridges in response to multi-parameter damages caused by human-induced vibrations.

The XGBoost algorithm operates on the principle of minimizing the target function during training. It achieves this by utilizing a second-order Taylor expansion and under-

going multiple iterations of the loss function. The objective is to reach the minimum of the target function, which occurs when the derivative of the target function equals zero. Consequently, this process yields the optimal prediction model.

SVR is widely utilized for solving regression problems. It operates as a non-probabilistic algorithm. By employing a kernel function, the data undergo mapping to a high-dimensional space, wherein the training data's maximum interval and the optimal hyperplane are established to construct the regression model.

The ANN, also known as Multilayer Perceptron (MLP), utilizes the backpropagation algorithm for training data. By inputting signals, the network calculates results and compares them with the true values to determine errors. Subsequently, weights are adjusted through backpropagation in accordance with these errors to minimize them. The structure of an ANN typically consists of an input layer, a hidden layer, and an output layer. The simplest form of an ANN includes only a single hidden layer.

2.3.2. Hyperparameter Adjustment and Optimization

During training and prediction, multiple hyperparameters of the machine learning model must be configured [20–23], with the hyperparameter values closely linked to the prediction performance. In this regard, when performing hyperparameter adjustment and optimization for the aforementioned three algorithms: SVR, XGBoost, and ANN, the authors employed the Tree-structured Parzen Estimator (TPE) method for SVR and XGBoost, and the Grid Search method for ANN. TPE operates on the basis of Bayesian principles. By continuously optimizing and iterating the specified target function and supplementing sampling points with expected improvements, it identifies parameter combinations that yield the most significant enhancement for subsequent sampling points, thus determining the most suitable hyperparameter values. On the other hand, Grid Search considers all possible hyperparameter combinations, searching for the combination that yields the best output results for the model, thereby concluding the hyperparameter optimization process.

2.3.3. Model Construction Procedure

This article proposes a machine learning-based method for swiftly predicting the comfort level of suspension footbridges amidst multi-parameter damages. This method hinges upon establishing a machine learning model capable of processing inputs related to crowd density, main cable damage coefficient, hanger damage coefficient, and steel longitudinal beam damage coefficient, with the output being vertical peak acceleration. The damage coefficient signifies the ratio between the difference in cross-sectional areas pre- and post-damage and the cross-sectional area before damage occurrence. Regarding the input and output data required for the model's training and validation sets, input data were obtained via random sampling utilizing the Monte Carlo method, while output data were derived from the Midas Civil finite-element model for dynamic response calculation, according to the sampling outcomes from the input data. Suitable algorithms were employed for hyperparameter adjustment and optimization, and three distinct machine learning algorithms were selected for model training and validation. Subsequently, the performance of these models was evaluated using performance indicators, with the model exhibiting the best performance being chosen as the final comfort level evaluation model. Finally, the measured bridge population density, main cable, sling, steel girder damage, and measured vertical peak acceleration were compared with the predicted value of the machine learning model to verify the feasibility of the machine learning model. The detailed procedure is illustrated in Figure 3 below.

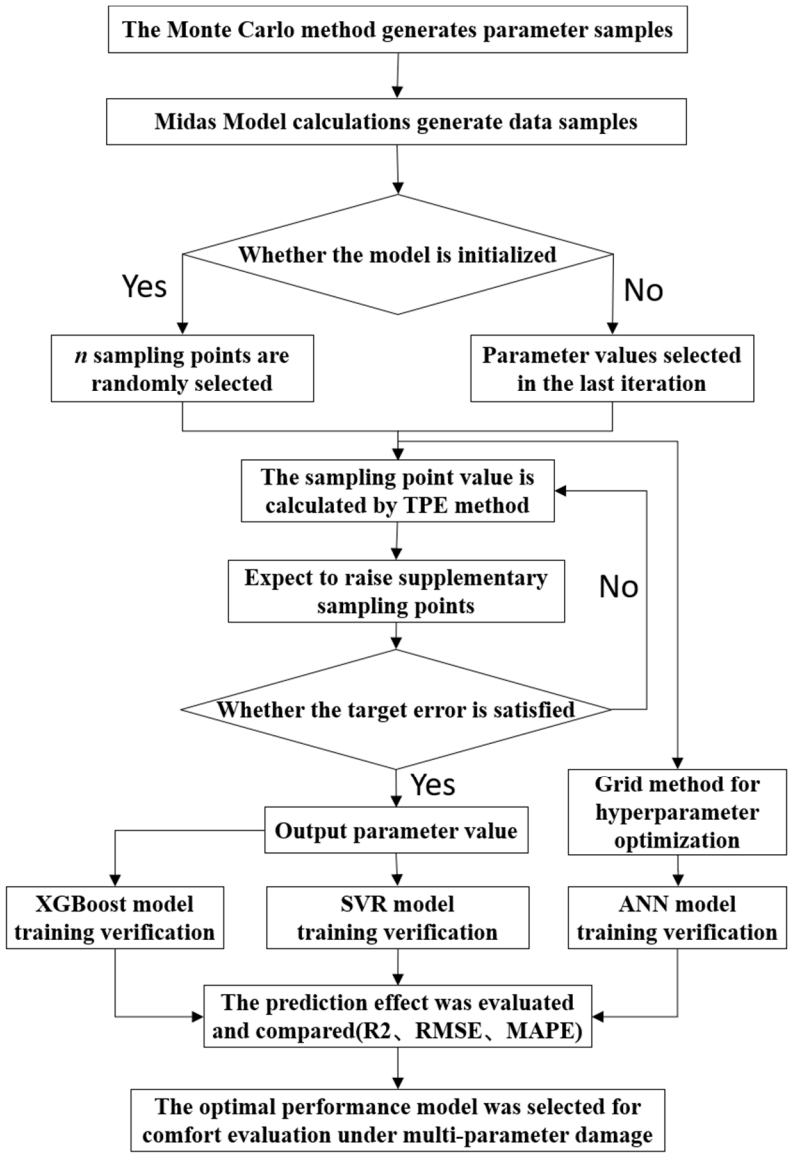

Figure 3. Model construction procedure.

3. Project Application

3.1. Project Overview

The Yangjiadong Suspension Bridge was constructed in 1997 and is situated at the Liangtan Wharf of Nuanshui Town, Rucheng County, Chenzhou City. The actual bridge is shown in Figure 4. This bridge employs a steel-cable suspension structure with a wooden bridge surface. Upon conducting on-site measurements, the material parameters and structural characteristics of the bridge were recorded, as depicted in Figure 5. The total length of the bridge spans 207.48 m, with the main beam extending over 125.09 m and the bridge surface measuring 2.7 m in width. For the main cable, four steel strands with specifications of Strand 1860 and a diameter of 32 mm are utilized, while 35 steel strands of the same specification and a diameter of 14 mm serve as hangers on each side. The steel longitudinal beams consist of five sheets of I-shaped steel fabricated from Q345 material, spaced at intervals of 0.65 m, and are covered with wooden boards approximately 80 mm-thick. The steel cross-beams comprise 35 sheets of I-shaped steel, also made from Q345 material, with intervals between them measuring 3.62 m. The Yangjiadong Suspension Bridge plays a crucial role as a traffic artery for local residents. Investigating the impact

of stiffness damage on the bridge's main components on its response to human-induced vibrations and evaluating the resulting comfort level hold significant practical importance.

(**a**) (**b**)

Figure 4. Yangjiadong Suspension Bridge actual bridge graph. (**a**) Elevation and (**b**) plan.

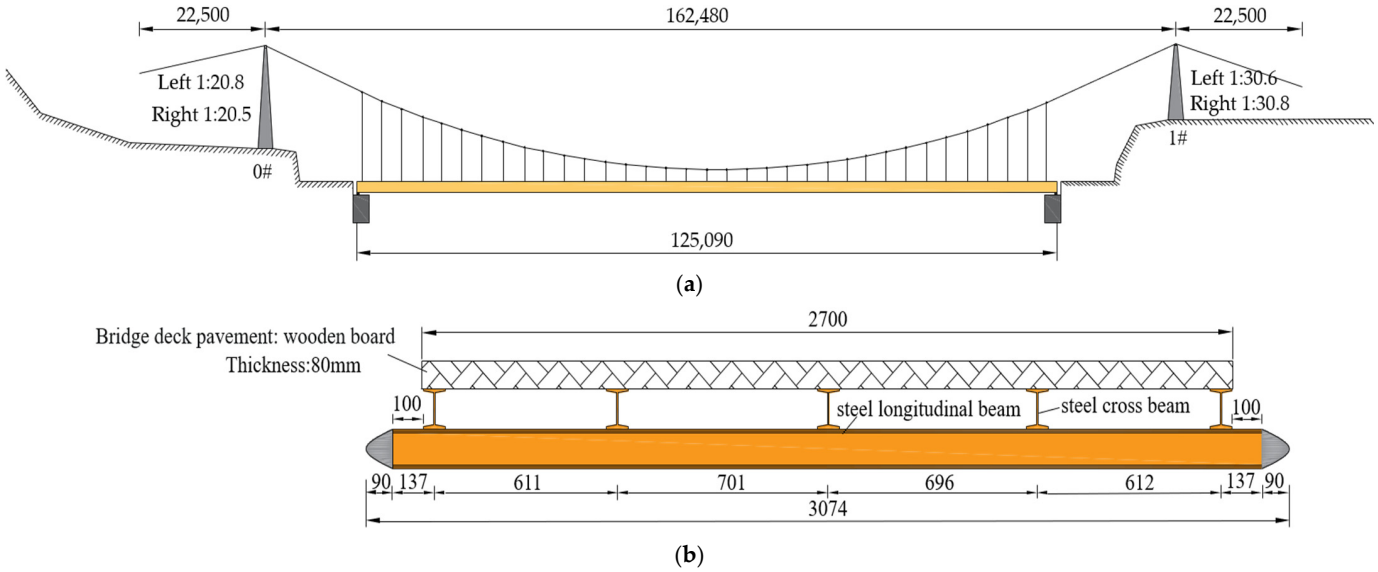

Figure 5. Structural diagram of the suspension footbridge (unit: mm). (**a**) Elevation view and (**b**) cross-sectional view of the steel beam.

3.2. Finite-Element Model

Based on the data gathered on site, we utilized Midas Civil to construct the finite-element model. During this process, we designated the main cable and hanger as cable elements, while the steel longitudinal beam, steel cross-beam, and horizontal stiffening girder were assigned as beam elements. The wooden bridge surface rests atop the steel longitudinal beam, with consideration given solely to its weight. This weight is evenly distributed and applied to the steel longitudinal beam as a beam element load. Boundary conditions [11,24–28] were addressed through the following steps: Consolidation was performed on the bottom of the cable tower, and at both ends of the main cable. A fixed hinged support was employed on one end of the steel beam, while a movable one was utilized on the other end. Rigid connections were established between the main cable and the hanger, the hanger and the steel longitudinal beam, as well as between the cable tower and the main cable. Elastic connections were implemented at the joint between the steel longitudinal beam and the steel cross-beam. Restrictions along the bridge's direction were imposed by the main cable and the cable tower at the cable saddle section. The established finite-element model is depicted in Figure 6.

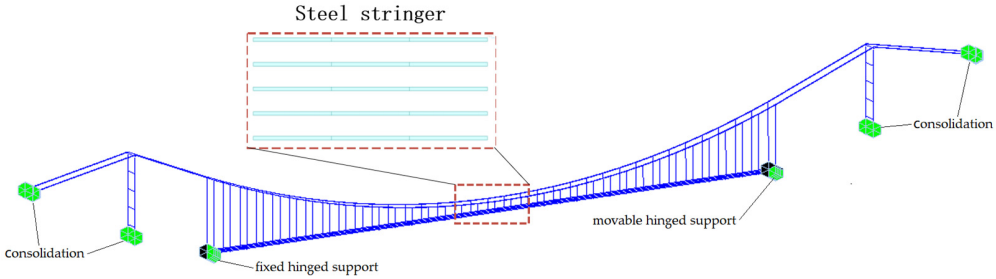

Figure 6. Finite-element model diagram.

4. Analysis of the Response to Human-Induced Vibrations and Evaluation of the Comfort Level

4.1. Analysis of the Influence of the Pedestrian Density

4.1.1. Frequency of Natural Vibration

The suspension footbridge's structure is relatively lightweight, and the pedestrians' weight significantly impacts the dynamic system of the human bridge structure [10]. Hence, when examining the effect of crowd density on the bridge's comfort level regarding vibrations, it is essential to analyze two scenarios: one with and one without consideration of pedestrian mass. This approach allows for evaluating the pedestrian mass's influence on the model calculation results. In cases where pedestrian mass is considered, the analysis involves incorporating the pedestrian mass into the bridge's self-weight. Initially, the first 50 modal orders were calculated, with the standard pedestrian mass set at 70 kg/person. Table 2 presents the outcomes of the first 10 modal orders' natural vibration frequencies under two conditions: with and without considering pedestrian mass, using a pedestrian density of 1 person/m^2 as an example. Taking into account pedestrian mass, the first 10 vibration modes are shown in Figure 7 below. In accordance with the German ENO3 norm [19], the model where the bridge's natural vibration aligned closely with the pedestrian's stride frequency was identified. Table 3 showcases the corresponding model, vibration order, natural vibration frequency, and the results of the vibration mode diagram. Subsequent analyses concerning the main cable, hanger, and steel longitudinal beam were conducted based on a crowd density of 1 person/m^2, factoring in the pedestrian mass in the model calculations.

4.1.2. Load Calculation

Based on the calculation method illustrated in Figure 1, reduction coefficients corresponding to different frequencies were determined. Subsequently, the vibration amplitude, frequency, equivalent pedestrian density, and reduction coefficient values were inputted into Formula (1) to derive the first-order simple harmonic wave load. The computed results are presented in Table 4. This approach for load calculation was then applied to analyze the subsequent main cable, hanger, and longitudinal steel beam.

Table 2. Natural vibration frequency (Hz) of the first 10 orders of the bridge.

Modal	Pedestrian Mass Counted	Vibration Mode Description	Pedestrian Mass not Counted	Vibration Mode Description
1	0.335	Antisymmetric Vertical Bend	0.345	Antisymmetric Vertical Bend
2	0.372	Symmetric Horizontal Bend	0.388	Symmetric Horizontal Bend
3	0.373	Vertical Bend	0.389	Vertical Bend
4	0.418	Antisymmetric Vertical Bend	0.430	Antisymmetric Vertical Bend
5	0.453	Symmetric Vertical Bend	0.469	Symmetric Vertical Bend
6	0.454	Vertical Bend	0.470	Vertical Bend
7	0.484	Symmetric Vertical Bend	0.498	Symmetric Vertical Bend
8	0.599	Symmetric Vertical Bend	0.616	Symmetric Vertical Bend
9	0.642	Antisymmetric Vertical Bend	0.664	Antisymmetric Vertical Bend
10	0.643	Vertical Bend	0.666	Vertical Bend

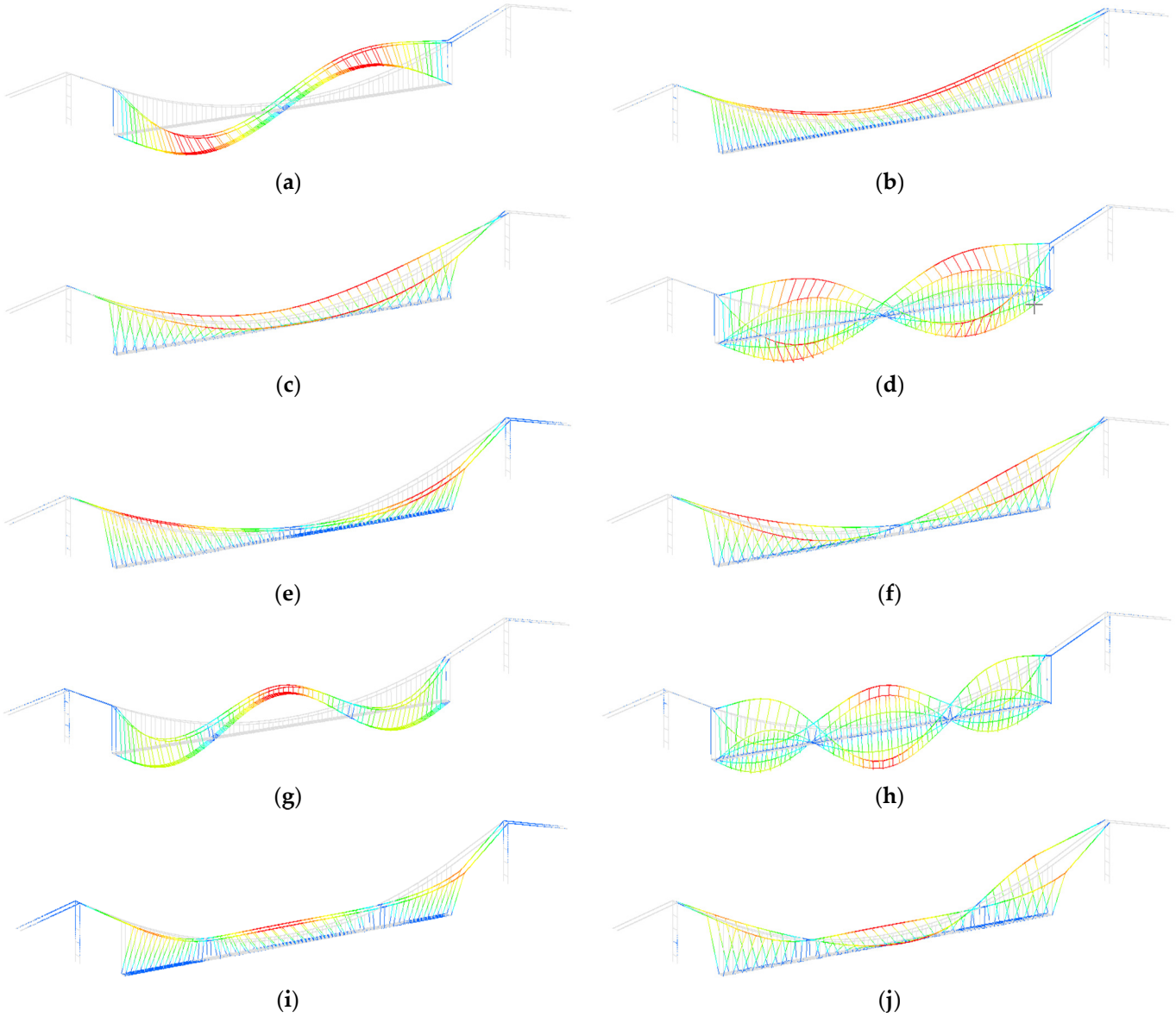

Figure 7. Vibration mode diagram. (**a**) Mode 1, (**b**) mode 2, (**c**) mode 3, (**d**) mode 4, (**e**) mode 5, (**f**) mode 6, (**g**) mode 7, (**h**) mode 8, (**i**) mode 9, and (**j**) mode 10.

Table 3. Vibration mode and natural vibration frequency of the bridge.

	Pedestrian Mass Counted				Pedestrian Mass not Counted			
	Modal	Vibration Order	Natural Vibration Frequency/Hz	Vibration Mode Diagram	Modal	Vibration Order	Natural Vibration Frequency/Hz	Vibration Mode Diagram
Horizontal Bend	8	3	0.599		8	3	0.616	
	14	4	0.848		14	4	0.870	
	18	5	1.062		18	5	1.089	
Vertical Bend	23	7	1.389		23	7	1.415	
	25	7	1.454		25	7	1.500	
	26	8	1.568		26	8	1.603	
	29	8	1.696		29	8	1.735	
	31	8	1.912		30	9	1.902	
	33	9	1.95		33	9	1.972	
	36	9	2.142		37	9	2.209	

Table 4. Pedestrian load model with different densities.

	Vibration Order	Crowd Mass Counted					Vibration Order	Crowd Mass not Counted			
		Pedestrian Density/Person/m^2						Pedestrian Density/Person/m^2			
		Coefficient	0.5	1	1.5	2		0.5	1	1.5	2
Horizontal Bend	3	cos(3.8*t*)	1.0	1.8	2.1	2.5	3	1.1cos(3.8*t*)	2.0cos(3.9*t*)	2.7cos(3.9*t*)	3.3cos(4.0*t*)
	4	cos(5.3*t*)	2.1	3.5	4.3	5.0	4	2.1cos(5.4*t*)	3.5cos(5.5*t*)	4.3cos(5.5*t*)	5.0cos(5.6*t*)
	5	cos(6.7*t*)	2.1	3.5	4.3	5.0	5	1.3cos(6.8*t*)	2.0cos(6.8*t*)	2.1cos(6.9*t*)	2.1cos(7.0*t*)
Vertical Bend	7	cos(8.7*t*)	4.8	8.2	10.0	11.5	7	3.3cos(8.4*t*)	10.3cos(8.9*t*)	9.4cos(8.6*t*)	12.3cos(8.7*t*)
	7	cos(9.1*t*)	7.5	12.8	15.6	18.1	7	5.6cos(8.8*t*)	15.7cos(9.4*t*)	13.8cos(9.0*t*)	17.0cos(9.1*t*)
	8	cos(9.9*t*)	11.6	19.9	24.4	28.2	8	12.2cos(10.0*t*)	22.1cos(10.1*t*)	28.5cos(10.2*t*)	34.4cos(10.3*t*)
	8	cos(10.7*t*)	16.3	27.9	34.2	39.5	8	16.5cos(10.7*t*)	28.2cos(10.9*t*)	34.5cos(11.1*t*)	40.0cos(11.2*t*)
	8	cos(12.0*t*)	16.5	28.2	34.5	39.9	9	16.5cos(12.2*t*)	28.2cos(12.0*t*)	34.5cos(12.1*t*)	40.0cos(12.2*t*)
	9	cos(12.3*t*)	16.5	28.2	34.5	39.9	9	12.3cos(13.5*t*)	28.2cos(12.4*t*)	34.5cos(12.6*t*)	40.0cos(12.5*t*)
	9	cos(13.5*t*)	13.0	22.3	27.3	31.5	9	9.7cos(13.7*t*)	12.8cos(13.9*t*)	10.0cos(14.1*t*)	5.2cos(14.3*t*)

4.1.3. Dynamic Response

After analyzing and calculating the maximum acceleration of various vibration orders based on different crowd densities, the results are depicted in Figure 8. It was observed that as crowd density increased, excluding crowd mass, the vibration response, as well as the horizontal and vertical peak accelerations, also increased. Specifically, at a crowd density of 2 person/m^2, the horizontal and vertical peak accelerations were 0.028 m/s^2 and 0.849 m/s^2, respectively. However, when the crowd mass was taken into account, the horizontal and vertical peak accelerations decreased to 0.021 m/s^2 and 0.612 m/s^2, respectively.

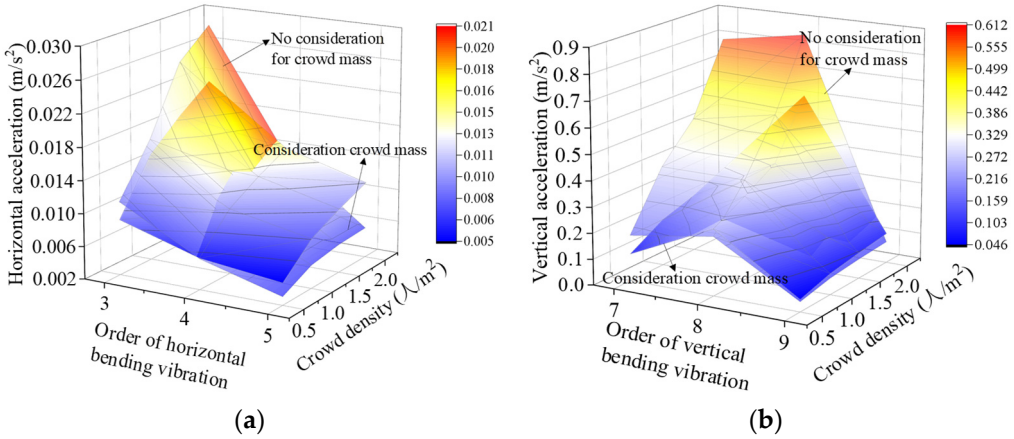

Figure 8. Maximum acceleration of various vibration orders. (**a**) Horizontal bend and (**b**) vertical bend.

4.2. Damage Analysis of Main Components

To investigate the impact of stiffness damage in the main cable, hanger, and steel longitudinal beam on the human-induced vibration comfort of bridge structures, we employed a sensitivity analysis method with a 1% increment. A substantial number of finite-element analyses were conducted, varying the cross-sectional area and elasticity modulus to simulate structural stiffness damage. This approach aids designers in consulting results pertaining to various degrees of structural damage for reinforcement purposes, thus offering valuable insights for the optimal design analysis of bridge structures.

4.2.1. Feature of Natural Vibration

We investigated the impact of single-component damage, including the main cable, hanger, and steel longitudinal beam, on the suspension bridge's response to human-induced vibrations by reducing the cross-sectional area of the component and the elasticity modulus of the material. Additionally, we sequentially reduced the cross-sectional area and elasticity

modulus of the main cable, hanger, and steel longitudinal beam by 1%. The resulting variations in the natural vibration frequency of the bridge's first-order model are depicted in Figure 9. Observations indicated that the natural vibration frequency of the bridge's first-order model decreased as the elasticity modulus of the main cable, hanger, and steel longitudinal beam was reduced. Specifically, when the cross-sectional area of the main cable decreased, the natural vibration frequency initially increased before declining. Conversely, reducing the cross-sectional area of the hanger and steel longitudinal beam led to a continuous decrease in the natural vibration frequency of the bridge's first-order model.

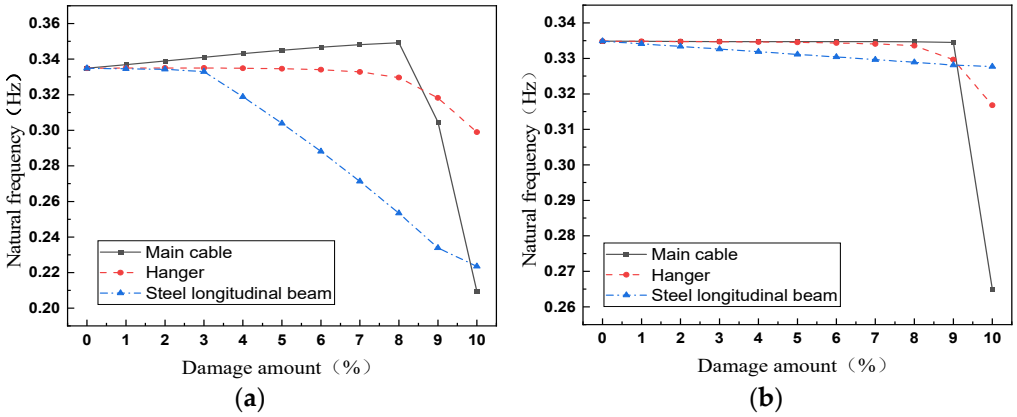

Figure 9. Influence of single structural damage on natural vibration frequency. (**a**) Cross-sectional area and (**b**) elasticity modulus.

4.2.2. Dynamic Response

We sequentially reduced the cross-sectional area and elastic modulus of the main cable, hanger, and steel longitudinal beam by 1%, as depicted in Figure 10, showcasing the variations in the acceleration response of the bridge's structure. The results illustrated in the figure reveal that as the cross-sectional area and elastic modulus of any component—be it the main cable, hanger, or steel longitudinal beam—declined, both the horizontal and vertical peak accelerations of the bridge's structure exhibited a consistent upward trend. When considering the variations in the natural vibration frequency of the first-order model, it became evident that peak acceleration experienced a surge concurrent with a sharp decrease in frequency.

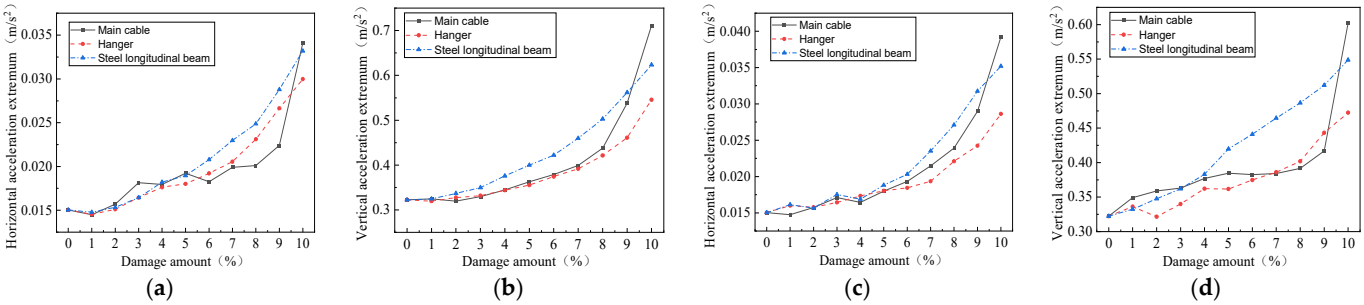

Figure 10. Influence of single structural damage on acceleration. (**a**) Cross-sectional area, (**b**) cross-sectional area, (**c**) elasticity modulus, and (**d**) elasticity modulus.

4.3. Evaluation of the Comfort Level

We selected peak acceleration as the indicator for evaluating comfort levels, following the criteria outlined in the German EN03 norm [19]. By examining various pedestrian densities and structural damages to the main cable, hanger, and steel longitudinal beam, we investigated how these factors affected the bridge's response to human-induced vibrations and, subsequently, evaluated its comfort level. The results indicated that higher

pedestrian densities led to increased peak accelerations and a decrease in structural comfort. Conversely, when accounting for crowd mass, peak acceleration decreased, resulting in improved comfort levels for the structure (see Figure 11).

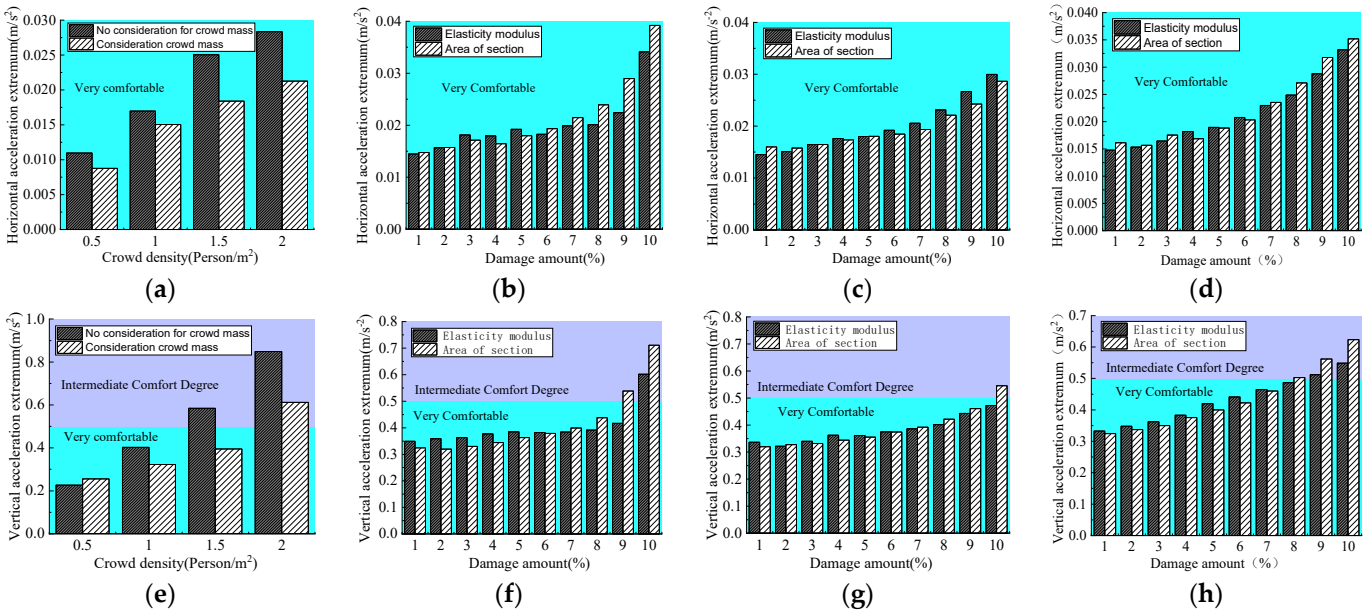

Figure 11. Evaluation of the comfort level under the influence of different factors. (**a**) Crowd density, (**b**) main cable, (**c**) hanger, (**d**) steel longitudinal beam, (**e**) crowd density, (**f**) main cable, (**g**) hanger, and (**h**) steel longitudinal beam.

The peak acceleration of the bridge structure increased with the proportion of damage, irrespective of whether the damage was attributed to the cross-sectional area of the main cable, hanger, and steel longitudinal beam, or to the elasticity modulus. Consequently, the comfort level of the bridge structure decreased. According to the aforementioned analytical findings, whether the damage arose from the cross-sectional area or the elasticity modulus of any single component—main cable, hanger, or steel longitudinal beam—when the damage proportion remained below 10%, the horizontal comfort level of the bridge structure consistently remained at the "very comfortable" level. Moreover, in the most adverse scenario, the vertical comfort level of the bridge structure was classified as the "intermediate comfort degree."

5. Comfort Level Prediction Based on Machine Learning

5.1. Analysis of Input Features

The establishment of machine learning models heavily relies on a substantial amount of sample data for support, and both the quantity and accuracy of this data have a significant impact on the accuracy of machine learning models. Therefore, it is paramount to acquire real-time damage coefficient and acceleration data of bridge structures and establish a data-driven repository and train predictive models to enhance their accuracy. Feng et al. [29] introduced a methodology that utilizes fiber optics in conjunction with sensors to continuously capture static and dynamic measurement data of bridges, thereby facilitating the development of a real-time bridge safety assessment system. Moreover, in another study, Feng et al. [30] proposed a technique for identifying optimal sensor layout positions and determining changes in the cross-sectional area through these sensors. The above research offers a means to procure the necessary real-time sample data for machine learning models.

In this article, finite-element simulation was used to obtain the data required by the machine learning model. We evaluated the comfort level of suspension footbridges against human-induced vibrations, considering the joint influence of multi-parameter damages. We

replaced component damages in actual engineering with the aforementioned cross-sectional damages for analysis and adopted machine learning methods to establish a surrogate model for prediction and evaluation. The crowd density, main cable damage coefficient, hanger damage coefficient, and steel longitudinal beam damage coefficient served as inputs, while vertical peak acceleration served as the output. Assuming that all parameters follow an even distribution within the specified value range, the Monte Carlo method was utilized for the sampling and combination of various parameters, resulting in 150 sample points. These data samples were then divided into a training set and a validation set at a ratio of 7:3. The *RMSE*, *MAPE*, and R^2 were used as evaluation indicators for the established surrogate model. Using the results of the sampled points calculated by Midas Civil software (version 2021), a data driving library was created. Initially, the correlation between various input and output parameters was analyzed. Figure 12 illustrates the heatmap of this correlation. The data in the map indicate a consistent degree of correlation between parameter variations and vertical peak accelerations across various structures. Among these data, the main cable, as the primary load-bearing component, exhibited the highest correlation (R^2 = 0.49), followed by structural parameters of the hanger and steel longitudinal beam.

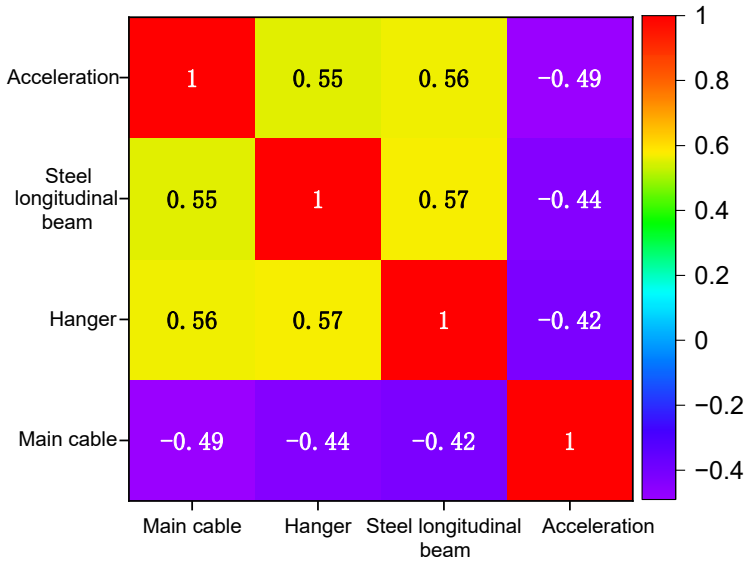

Figure 12. Heat map of the correlation between input and output parameters of the model.

5.2. Model Comparison and Analysis

Based on the damage coefficient, we examined the impact of various structural parameters on damage. Inputs included crowd density and damage coefficients of different structures, with vertical peak acceleration as the output, used to adjust and optimize the model's hyperparameters. The optimal hyperparameter settings for the XGBoost model were as follows: the total number of decision trees involved was 930, with a column sampling proportion of 0.71, a gamma value of 0.04, a learning rate of 0.10, a maximum depth of 100, a sub-sample proportion of 0.82, and a minimum sub-segment weight of 4.0. For the SVR model, the hyperparameter optimization yielded a value of C as 20.0, epsilon as 0.03, and gamma as 1.2. Meanwhile, for the ANN model, the optimization resulted in two hidden layers, each with 100 neurons, and a learning rate of 0.005.

Model training and validation were conducted based on the results of hyperparameter adjustment and optimization. Figure 13 shows scatter diagrams depicting the prediction results of the training and validation sets for the three models. Evaluation indicators were utilized for comparative analysis. For the XGBoost model, the *RMSE*, *MAPE*, and R^2 values for the training set were 0.01, 0.02, and 0.99, respectively, while for the validation set, they were 0.03, 0.02, and 0.94, respectively. Similarly, for the SVR model, the *RMSE*, *MAPE*, and R^2 values for the training set were 0.03, 0.02, and 0.98, respectively, and for the validation set, they were 0.04, 0.02, and 0.96, respectively. Regarding the ANN model, the *RMSE*,

MAPE, and R^2 values for the training set were 0.02, 0.02, and 0.99, respectively, while for the validation set, they were 0.03, 0.02, and 0.98, respectively. These three machine learning models, established on this basis, contributed to high precision in predicting the vertical acceleration of the structure, enabling quick evaluation of the structure's comfort level.

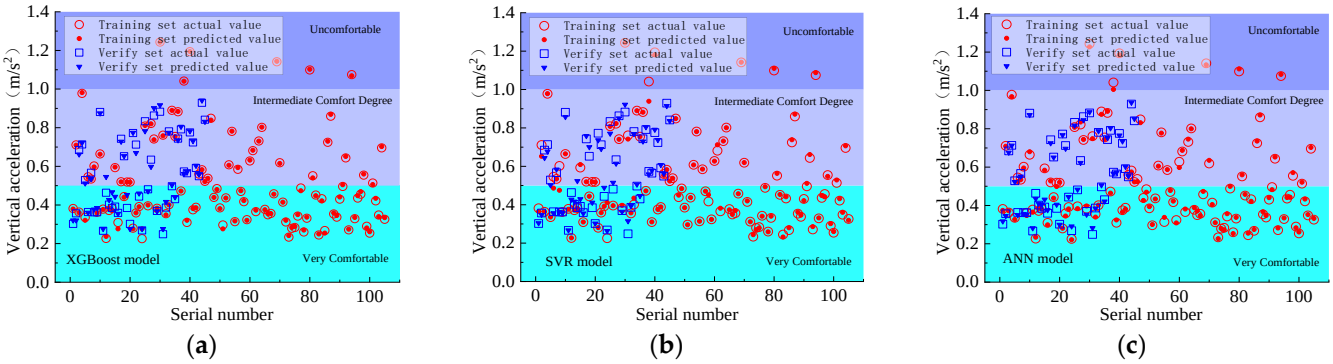

Figure 13. Effect of comfort level prediction of the three machine learning models. (**a**) XGBoost model, (**b**) SVR model, and (**c**) ANN model.

5.3. Comparison of Generalization Performance of Models

In the preceding analysis, three models, evaluating the comfort level in the event of multi-parameter damages, were established based on machine learning algorithms. Considering the susceptibility of the suspension footbridge to external environmental influences during future operation, which may lead to more severe cross-sectional losses and other structural damages, it is imperative to assess the generalization performance of predicting the bridge structure's comfort level under various parameter-based damages in future operations. Differing from the sample points utilized for training and validation, the Monte Carlo method was also employed to sample crowd density, main cable damage, hanger damage, and steel longitudinal beam damage, with ten sample points randomly selected. The outcomes of these sample points were obtained through simulated calculations using finite-element software, allowing for comparison with the predicted values of the model to evaluate the generalization performance of three machine learning-based models for assessing the comfort level based on multi-parameter damages in future operations. Figure 14 illustrates the comparison of the prediction effects of the three models, while Figure 15 depicts the relative error between the predicted values of the ANN model and the calculated values of the finite-element model. It can be observed that the fitted line of the ANN model's sample points closely approximated the optimal fitted line, with a relative error lower than 5%, indicating that the ANN model's prediction effectiveness was superior. Furthermore, its generalization performance in predicting capacity for future operations was also exemplary. Considering the precision of the ANN model's validation set, it was ultimately selected as the model to predict and evaluate the comfort level in the suspension footbridge, considering multi-parameter damages with the influence of human-induced vibrations.

5.4. Comparison of Actual Measured Data

Three magnetoelectric vibration sensors were employed and positioned at intervals corresponding to 1/4, 1/2, and 3/4 of the bridge's span, respectively. Upon reaching a crowd density of 0.5 people/m^2 on the anticipated bridge during a specific time period, the accelerations of the bridge structure were recorded over a duration of ten minutes. The details regarding the measurement instrument model, serial numbers, and arrangement of measurement points are provided in Table 5 below. The vertical acceleration data for the physically measured bridge can be observed in Figure 16.

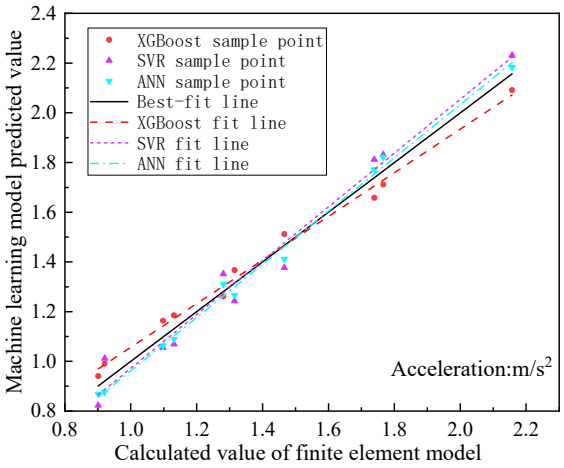

Figure 14. Comparison of the generalization performances of the three machine learning models.

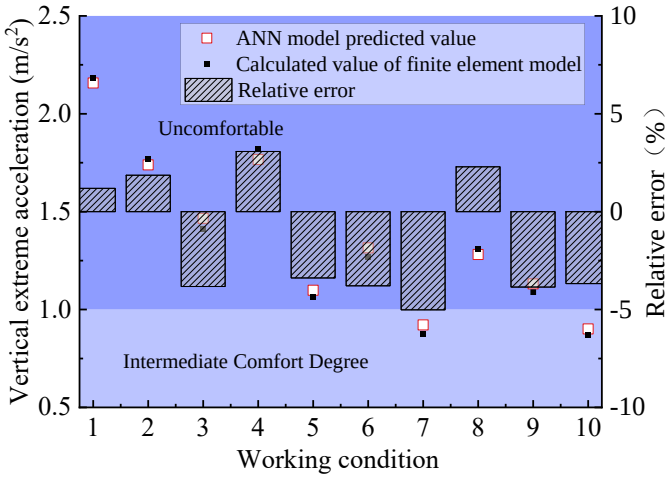

Figure 15. Prediction error of the ANN model.

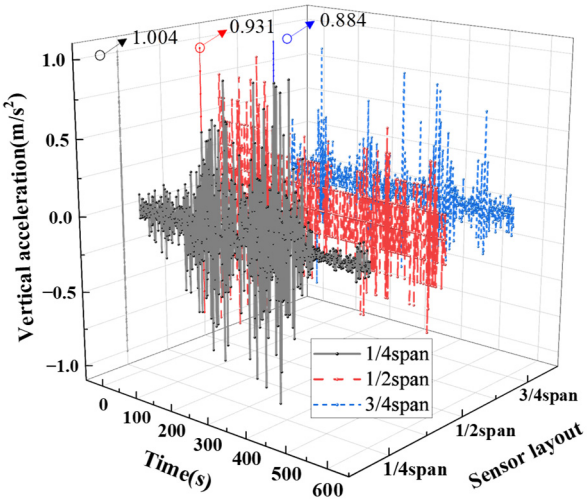

Figure 16. Actual measured results of the acceleration (vertical).

Through on-site testing and calculations, it was determined that the measured coefficient of the main cable, hanger, and steel longitudinal beam was 0.87, indicating a corresponding damage coefficient of 0.13. When the actual crowd density at the site was 0.5 people per square meter, the maximum vertical acceleration recorded was 1.004 m/s^2.

However, finite-element simulation and analysis revealed that the maximum vertical acceleration was 1.064 m/s^2, as illustrated in Figure 17.

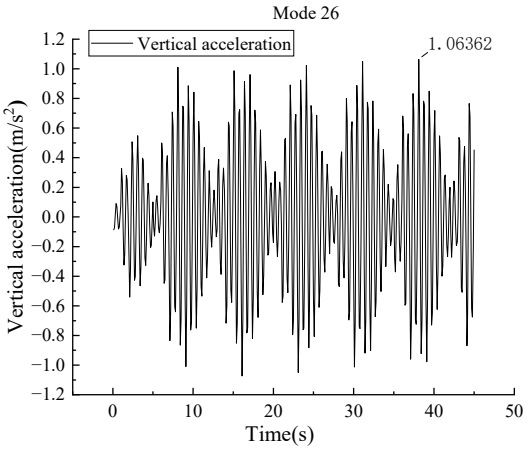

Figure 17. Time course diagram of the maximum acceleration (vertical).

Table 5. Sensor models and serial numbers.

Instrument Name	Instrument Model	Instrument Number	Instrument Serial Number
Magnetoelectric Vibration Sensor	2D001V	1	SB/LZ-JC-2020021-3
	2D001V	1	SB/LZ-JC-2020021-5
	2D001V	1	SB/LZ-JC-2020021-8

6. Conclusions

(1) This study focused on Yangjiadong's suspension footbridge as the research subject, revealing that the base frequency of the bridge structure was relatively low and exhibited significant flexibility. Comparatively, when considering crowd mass, the comfort level improved. On-site measurements showed a damage coefficient of 0.13 for the main cable, hanger, and steel longitudinal beam. With a crowd density of 0.5 people/s^2, the maximum measured acceleration was 1.004 m/s^2, resulting in an "uncomfortable" comfort level. Consequently, it is recommended to restrict pedestrian numbers to maintain the bridge's comfort level within an acceptable range and prevent accidents.

(2) We selected three commonly used machine learning models, after comparative analysis, to assess comfort levels, culminating in an ANN-based model designed to evaluate suspension footbridge comfort levels based on multi-parameter damages and human-induced vibrations. Demonstrating high precision, the model's validation set yielded an RMSE, MAPE, and R^2 of 0.03, 0.02, and 0.98, respectively. Future operational comfort level predictions exhibited an error rate within 5%, indicating a robust generalization performance. This model serves as a valuable reference for subsequent bridge structure comfort level monitoring. In future studies, a wider range of machine learning models can be explored, and more parameters can be considered to develop more general prediction methods with higher accuracy and robustness.

(3) On-site measurements of the main cable, hanger, and steel longitudinal beam revealed a damage coefficient of 0.13. With a crowd density of 0.5 people/m^2, the maximum measured acceleration was 1.004 m/s^2, while the ANN model predicted 1.098 m/s^2, with a 9.4% error. This suggests the model's utility for rapid bridge structure comfort level evaluations.

Author Contributions: S.Z., methodology; X.T., writing—original draft; Y.D., investigation. All authors have read and agreed to the published version of the manuscript.

Funding: This research was funded by the Special Project for the Construction of Innovative Provinces in Hunan Province (Grant No. 2019RS1059).

Data Availability Statement: The relevant data in this study can be obtained from the corresponding author.

Conflicts of Interest: Author Yongjun Du was employed by the company Shanxi Xingtong Engineering Consulting Co., Ltd. The remaining authors declare that the research was conducted in the absence of any commercial or financial relationships that could be construed as a potential conflict of interest.

References

1. Živanović, S.; Pavic, A.; Reynolds, P. Vibration serviceability of footbridges under human-induced excitation: A literature review. *J. Sound Vib.* **2005**, *279*, 1–74. [CrossRef]
2. Harper, F.C.; Warlow, W.J.; Clarke, B.L. *Walking on a Level Surface. National Building Studies: Research Paper*; HMSO: London, UK, 1961; p. 32.
3. Harper, F.C. The mechanics of walking. *Res. Appl. Ind.* **1962**, *15*, 23–28.
4. Wright, D.T.; Green, R. Highway Bridge Vibrations: Part II, Ontario Test Programme. Master's Thesis, Department of Civil Engineering, Queen's University, Kingston, ON, Canada, 1964.
5. Lai, E.; Gentile, C.; Mulas, M.G. Experimental and numerical serviceability assessment of a steel suspension footbridge. *J. Constr. Steel Res.* **2017**, *132*, 16–28. [CrossRef]
6. Feng, X.; Chen, G.S.; Hulsey, J.L.; Dolan, J.D.; Dong, Y.T. Ambient loading and modal parameters for the Chulitna River Bridge. *Adv. Struct. Eng.* **2016**, *19*, 660–670.
7. Feng, P.; Jin, F.F.; Ye, L.P.; Zhu, S.Y. Quantification of pedestrian's comfort level and dynamic properties of footbridge vibration based on in-situ measurement. *J. Vib. Eng.* **2013**, *26*, 545–553.
8. Han, H.X.; Zhou, D.; Ji, T.J.; Zhang, J.D. Modelling of lateral forces generated by pedestrians walking across footbridges. *Appl. Math. Model.* **2021**, *89*, 1775–1791. [CrossRef]
9. Yu, Z.H.; Liu, H.C. Vibration performance and comfort evaluation of Xunjiang cable-stayed bridges under combined action of wind-vehicle-pedestrian loadings. *J. Railw. Sci. Eng.* **2023**, *20*, 1425–1432. [CrossRef]
10. Liu, F.; Qin, G.; Ma, M.; Zhang, Q.; Song, T.; Zhang, G.M. Analysis and test of human induced vibration of pedestrian suspension bridge. *J. Build. Struct.* **2023**, *44*, 72–82. [CrossRef]
11. Zhang, Y.L.; Wang, C.; Zhang, X.; Wang, A.Y.; Li, Y.S. Human-induced vibration analysis and pedestrian comfort evaluation for suspension footbridge with different hunger systems. *J. Jilin Univ. (Eng. Technol. Ed.)* **2022**, *52*, 2644–2652. [CrossRef]
12. Wan, T.B. Key techniques of design of special shape glass floor suspension bridge over Zhangjiajie grand canyon. *Bridge Constr.* **2017**, *47*, 6–11.
13. Wang, Z.F.; Li, X.J.; Yi, J.; Li, Q.S. Human-induced vibration and optimal control of long-span glulam arch bridges. *China Civ. Eng. J.* **2021**, *54*, 79–94.
14. Bayane, I.; Leander, J.; Karoumi, R. An unsupervised machine learning approach for real-time damage detection in bridges. *Eng. Struct.* **2024**, *308*, 117971. [CrossRef]
15. Chen, Y.; Zeng, J.; Jia, J.P.; Jabli, M.; Abdullah, N.; Elattar, S.; Khadimallah, M.A.; Marzouki, R.; Hashmi, A.; Assilzadeh, H. A fusion of neural, genetic and ensemble machine learning approaches for enhancing the engineering predictive capabilities of lightweight foamed reinforced concrete beam. *Powder Technol.* **2024**, *440*, 119680. [CrossRef]
16. Dong, C.Z.; Bas, S.; Catbas, F.N. Investigation of vibration serviceability of a footbridge using computer vision-based methods. *Eng. Struct.* **2020**, *224*, 111224. [CrossRef]
17. Cao, L.; Zhou, H.L.; Lu, F.M. Intelligent recognition algorithm for human dynamic parameters of walking load. *Eng. Mech.* **2023**, *40*, 1–12. [CrossRef]
18. Chen, D.Y.; Wu, J.; Yan, Q.S. A novel smartphone-based evaluation system of pedestrian-induced footbridge vibration comfort. *Adv. Struct. Eng.* **2019**, *22*, 1685–1697. [CrossRef]
19. *EN 03*; Design of Footbridges: Guideline. Research Found for Coal and Steel: Aachen, Germany, 2008.
20. Zhang, X.Y.; Dai, C.Y.; Li, W.Y.; Chen, Y. Prediction of compressive strength of recycled aggregate concrete using machine learning and Bayesian optimization methods. *Front. Earth Sci.* **2023**, *11*, 1112105. [CrossRef]
21. Wei, Y.Z.; Ji, R.Q.; Li, Q.F.; Song, Z.M. Mechanical Performance Prediction Model of Steel Bridge Deck Pavement System Based on XGBoost. *Appl. Sci.* **2023**, *13*, 12048. [CrossRef]
22. Silva, V.P.; Carvalho, R.D.A.; Rêgo, J.H.D.S.; Evangelista, F., Jr. Machine Learning-Based Prediction of the Compressive Strength of Brazilian Concretes: A Dual-Dataset Study. *Materials* **2023**, *16*, 4977. [CrossRef]

23. Tan, B.K.; Wang, D.; Shi, J.L.; Zhang, H.Q. Temperature field prediction of steel-concrete composite decks using TVFEMD-Stacking ensemble algorithm. *J. Zhejiang Univ. Sci. A*. 2024, *in press*. Available online: https://jzus.zju.edu.cn/iparticle.php?doi=10.1631/jzus.A2300441 (accessed on 26 April 2024).
24. Pan, Q.; Yan, D.H.; Yi, Z.P. Form-Finding Analysis of the Rail Cable Shifting System of Long-Span Suspension Bridges. *Appl. Sci.* **2018**, *8*, 2033. [CrossRef]
25. Li, J.L.; Liu, X. Human-Induced Vibration Analysis and Reduction Design for Super Long Span Pedestrian Arch Bridges with Tuned Mass Dampers. *Appl. Sci.* **2023**, *13*, 8263. [CrossRef]
26. Yang, S.; Yang, J.R.; Li, R. Evaluation of Pedestrian Comfort for a Footbridge with Hinged Piers. *Sustainability* **2023**, *15*, 9851. [CrossRef]
27. Zhou, J.H.; Huang, Y.Q.; Liu, A.R. Walking comfort analysis and vibration control of bridge with curved beam and inclined arch. *Eng. Mech.* **2022**, *39*, 214–220.
28. Gattulli, V.; Potenza, F.; Piccirillo, G. Multiple tests for dynamic identification of a reinforced concrete multi-span arch bridge. *Buildings* **2022**, *12*, 833. [CrossRef]
29. Feng, X.; Hulsey, J.L.; Balasubramanian, R. Fiber optic health monitoring and temperature behavior of bridge in cold region. *Struct. Control Health Monit.* **2017**, *24*, e2020.
30. Feng, X.; Hulsey, J.L.; Chen, G.S.; Xiang, Y.J. Optimal static strain sensor placement for truss bridges. *Int. J. Distrib. Sens. Netw.* **2017**, *13*, 1550147717707929.